

# The Design and Scale-Up of Multiple-Impeller Fermenters for Liquid Film Controlled Processes

KUI – 10/2013  
Received October 11, 2012  
Accepted February 4, 2013

L. Labík, T. Moucha,\* and M. Kordač

Institute of Chemical Technology Prague, Chemical Engineering Dept.,  
Technická 5, 166 28 Praha 6, Czech Republic

Mechanically agitated gas-liquid contactors are frequently used in the chemical, food and biochemical industries as fermenters and as hydrogenation or chlorination reactors. However wide is the usage of such vessels, their design is not based on chemical engineering data, but is still rather empirical. Thus, it is highly desirable to have a tool for the rational design of agitated gas-liquid contactors that is based on fundamental chemical engineering parameters that are transferable to other systems and operating conditions. Focusing on liquid film-controlled processes and using the data from fermenters of different scales, we develop  $k_L a$  correlations that are suitable for scale-up.

First, we discuss how to determine the proper experimental  $k_L a$  values, which are not distorted by other equipment parameters as is the gas residence time. We demonstrate the possible  $k_L a$  distortion on the pilot-plant experimental data by comparing the results obtained by two different experimental techniques. Further, we present physically correct  $k_L a$  data for fully non-coalescent (sodium sulphate solution) batch. The data are presented both for laboratory and pilot-plant fermenters. We identify the process parameters, the values of which are dependent on the vessel scale when operated under the same power input per volume, and, using these parameters, we develop common  $k_L a$  correlations suitable to describe the data for various scales of the vessel.

The correlations developed reduce the uncertainty in predicting the volume of industrial scale fermenters from almost 1/2 to 1/4 of their total volume, thereby enabling significant reductions in both the initial costs, and operating costs.

Key words: *Fermenter, mass transfer, mass transfer correlations, mixing, multiple-impeller, scale-up, volumetric mass transfer coefficient*

## 1. Introduction

Mechanically agitated gas-liquid contactors are frequently used in chemical, food and biochemical industries as fermenters and as hydrogenation or chlorination reactors. However wide is the usage of such vessels, their design is not based on chemical engineering data but is still rather empirical. Several papers point out the need of rational design based on fundamental chemical engineering parameters. Sentences such as “In fermentation processes where oxygen transfer is the rate limiting step, correct measurement and subsequent estimation of the volumetric mass transfer coefficient is a crucial step in the design procedure of bioreactors”<sup>1</sup> or “Understanding of the mass transfer behaviour in bioreactors for gas treatment will result in improved reactor designs, reactor operation, and modelling tools, which are important to maximize efficiency and minimize costs”<sup>2</sup> represent motivation for further work in this field. We add that, in the case of bioreactors, the gas-liquid mass transfer is the rate-controlling step

not only in the oxygen supply from gas but also in the CO<sub>2</sub> removal from liquid. If the key parameter in such situations – volumetric mass transfer coefficient – is determined separately, it can be transferred to other systems and operating conditions (unlike the oxygen transfer rate – OTR values, which differ according to gas solubility and the dissolved gas concentration in different fermentation broths).

In the equation for the oxygen transfer rate

$$\text{OTR} = k_L a \cdot (c_L - c_L^*) \quad (1)$$

the fundamental data – mass transfer coefficient  $k_L$  and interfacial area  $a$  – can be used conveniently in the form of a more integral parameter – volumetric mass transfer coefficient –  $k_L a$ . This parameter can be categorized to the data for i) coalescent, ii) non-coalescent and iii) viscous batches. Such categorization is generally accepted. For instance, *Takahashi and Nienow*<sup>3</sup> mentioned the significance of determining the coalescence rate, which belongs to parameters from which mass transfer rates can be formulated.

In literature, we can find various approaches to  $k_L a$  determination in gas-liquid systems. With respect to the theoretical predictions, for several decades articles have been presented, which support construction of  $k_L a$  from hydro-

\* Corresponding author: Doc. Dr. Ing. Tomáš Moucha,  
e-mail: [tomas.moucha@vscht.cz](mailto:tomas.moucha@vscht.cz)

dynamic description. Such articles include for instance those by *Timson and Dunn*,<sup>4</sup> dealing with the dependency of mass transfer rate on the shear and on the surface tension, by *Okawa et al.*<sup>5</sup> dealing with the bubble size prediction, by *Del Castillo*<sup>6</sup> dealing with bubble coalescence (even suggesting the different coalescence mechanisms at low and high relative velocities of bubbles and liquid); by *Talaia*<sup>7</sup> who precisely described terminal velocities of bubbles. The literature data can be used in combinations, e.g., Talaia's precise velocities with the model of bubble breakage by *Prince and Blanch*,<sup>8</sup> who originally published in their work the equation for bubble rising velocity being "strictly applicable only to uncontaminated bubbles with mobile gas-liquid interfaces" or the model by *Kawase and Moo-Young*,<sup>9</sup> where the rising velocity is supposed to be constant about  $0.265 \text{ m s}^{-1}$  for all cases modelled.

For the gas-liquid dispersions with mechanical agitation, the theoretical quantification of  $k_L a$  in mechanically agitated vessels based on hydrodynamic principles is less frequent compared to bubble columns. This is due to more complex hydrodynamic conditions in mechanically agitated dispersions. Recently, the comprehensive article on the CFD study of a mechanically agitated dispersion has been written by *Ranganathan and Sivaraman*,<sup>10</sup> where the overview of other articles dealing with the topic is also given. Such studies, however, need too large computational time and, therefore, some simplifications need to be made. In the case of the work of *Ranganathan and Sivaraman*<sup>10</sup> the results were obtained using only "two bubble velocity groups to reduce computational cost". As the consequence of the simplification, they could report the agreement with the experimental data by *Alves*<sup>11</sup> only for the  $k_L a$  data up to  $0.06 \text{ s}^{-1}$ , while the  $k_L a$  measured in non-coalescent batches reached slightly above  $1 \text{ s}^{-1}$  (see the results in section 4.1.3.1). The survey of the uncertainties and obstacles in the theoretical prediction of  $k_L a$  data in agitated dispersion has been fairly described by *Martin et al.*<sup>12</sup>

For reasons discussed above, for mechanically agitated dispersions the empirical  $k_L a$  correlations are often presented in literature. Numerous literature  $k_L a$  data are described by the classical correlation based on the theory of isotropic turbulence:

$$k_L a = K_1 P^{K_2} v_s^{K_3} \quad (2)$$

*Van't Riet*<sup>13</sup> categorized the literature data for water and electrolyte solutions, and summarized them into the equations:

$$k_L a = 0.026 P^{0.4} v_s^{0.5} \quad (3)$$

for water, and

$$k_L a = 0.002 P^{0.7} v_s^{0.2} \quad (4)$$

for electrolyte solutions.

The category of viscous liquids is studied separately by *Herbst et al.*<sup>14</sup> who also presented an overview of literature correlations for it, or by *Nocentini et al.*<sup>15</sup> who found the  $k_L a$  dependencies

$$k_L a = 0.0015 P^{0.59} v_s^{0.55} \quad (5)$$

for water, and

$$k_L a \approx P^{0.62} v_s^{0.4} (\eta/\eta_w)^{-1.17} \quad (6)$$

for glycerine solutions.

While  $K_2$  value is low for coalescent systems and practically all literature data lie within the interval  $0.6 \pm 0.05$ , the exponent for non-coalescent batches varies significantly. Further  $K_2$  values for non-coalescent batches presented in literature are given in Table 1.

Table 1 – Power factors  $K_2$  defined by equation 2 found for non-coalescent batch by various authors

Tablica 1 – Faktori snage  $K_2$  definirani jednačbom 2, iz različitih literaturnih izvora, za šaržu bez koalescencije (spajanja)

| $K_2$       | Reference<br>Literatura                         |
|-------------|---|
| 0.9         | <i>Robinson and Wilke</i> <sup>16</sup>         |
| 0.946       | <i>Linek et al.</i> <sup>17</sup>               |
| 0.98        | <i>Puthli et al.</i> <sup>18</sup>              |
| 1.05        | <i>Pedersen et al.</i> <sup>19</sup>            |
| 1.2         | <i>Imai et al.</i> <sup>20</sup>                |
| 1.24        | <i>Linek et al.</i> <sup>21</sup>               |
| 1.28        | <i>Poizat et al.</i> <sup>22</sup>              |
| 1.24 – 1.32 | <i>Puskeiler and Weuster-Botz</i> <sup>23</sup> |

*Pedersen et al.*<sup>19</sup> categorized their  $k_L a$  results for coalescent and non-coalescent batches using the equation

$$k_L a = K_1 v_s^{0.4} f^{3K_2} \quad (7)$$

with  $K_2 = 0.654$  for water (coalescent batch) and  $K_2 = 1.05$  for  $0.26 \text{ M Na}_2\text{SO}_4$  solution (non-coalescent batch). So the value of  $K_2 = 1.05$  is included in Table 1 assuming that the  $f^3$  term is directly proportional to  $P$ , although it could not exactly be under aerated conditions.

The  $k_L a$  dependencies show large differences in  $K_2$  values for non-coalescent batches (from 0.7 to 1.32), which deserves the analysis of possible reasons. The  $k_L a$  data are measured by various experimental techniques, many of which produce physically incorrect  $k_L a$  data. The data in some cases can be corrected using more complex physical models of phases flow. To extract the proper value of the volumetric mass transfer coefficient from experimental OTR data, it is necessary to separate the driving force properly. To calculate the proper values of the driving force, various models of gas and liquid flow pattern have been suggested in literature. The flow models generally used for calculation of the driving force are perfectly mixed liquid phase combined with either piston flow or perfect mixing in gas. While the perfectly mixed liquid phase is usually a reasonable approximation, for the gas phase it is applicable only for coalescent systems in which the coalescence and redispersion of bubbles in the batch assure a perfect mixing of gas phase. For liquids containing substances that hinder or inhibit coalescence of bubbles in the batch, the model malfunctions give significantly undervalued  $k_L a$ .

To take the real behaviour of the gas phase into account, more sophisticated models of flow were used, such as plug

flow with axial dispersion (Nocentini et al.),<sup>15</sup> plug flow for large bubbles and perfect mixing for small bubbles (Pinelli)<sup>24</sup> or the model of two parallel series of perfect mixers with backflow, where the respective branches corresponded to the small and large bubbles (Havelka et al.).<sup>25</sup> Midoux et al.<sup>26</sup> used a model that starts from the initial gas bubble distribution produced by an agitator, and the concentration of absorbed species in the bubbles is calculated using their residence times. These more rigorous approaches are complex and hardly applicable for serial experiments even though the physically correct  $k_L a$  values can be obtained this way. Compare, for instance, Figs. 14 and 16 in the paper by Linek et al.,<sup>27</sup> where the correct  $k_L a$  data are obtained using the complex model of the series of perfect mixers with exchange flows in liquid and the plug flow with axial dispersion in gas.

Some techniques, however, are unable to provide physically correct  $k_L a$  data at all under a certain range of process conditions. The Start-up Method or the Classical Dynamic Method can serve as the examples of such techniques. In the Start-up Method, the mixing and aeration start at the beginning of each experiment, so under higher mixing intensities the major part of experiment (liquid saturation up to the final steady state) takes place in the start-up period, when the gas hold-up is formed. The resulting  $k_L a$  data are distorted significantly because the gas hold-up formation cannot be described with sufficient accuracy.<sup>17</sup> In the Classical Dynamic Method, the disturbance in gas is realized by a step concentration change at the gas inlet. Therefore, we should account for another possible limitation of liquid saturation rate – the rate of concentration change in gas itself; the original gas hold-up is washed out by the new one and, the concentration in the gas hold-up changes according to the time constant given by the gas residence time. Under higher  $k_L a$  values (achieved at higher mixing intensities), the concentration change in gas (higher gas hold-up wash out) is then slow, compared to gas-liquid mass transfer intensity, and the liquid, owing to the fast interfacial mass transfer, is almost in the equilibrium to gas at each moment, regardless of the exact value of  $k_L a$ . Under such conditions, the dynamic of gas hold-up washout (gas residence time  $\tau_c$ ) is measured through the liquid concentration-time profile, instead of the volumetric mass transfer coefficient  $k_L a$  (sometimes resulting in the principle change of the  $k_L a$  dependency on the impeller power from the rising trend to the decreasing one).<sup>17,21,28</sup> Such a situation is analogical to those generally considered in the case of chemical reactors: Typically, the reaction in the reactor is operating under either mass transfer limited or kinetically limited conditions.<sup>2</sup> Under kinetic limitation, a chemical reaction is slow, so the process is not limited by the interfacial mass transfer. Under such conditions, we can obtain no information on the mass transfer coefficient from the rate of the process.

To study the  $k_L a$  behaviour in fermenters, we first need to select a reliable experimental technique. We can consider the Dynamic Pressure Method (DPM) developed in our workplace earlier.<sup>29</sup> The physical accuracy of the  $k_L a$  data obtained by the DPM was verified earlier in laboratory scale vessel, and this method was also found suitable by other authors.<sup>1,30,31</sup> Carbajal and Tecante<sup>30</sup> compared Classical Dynamic Method with the DPM and concluded that

“In the Newtonian fluids the  $k_L a$  values obtained by the dynamic method were smaller than those from the DPM because the former is significantly more sensitive to the hydrodynamic conditions”; according to Gogate and Pandit,<sup>1</sup> “the dynamic pressure method appears most useful for industrial scale bioreactors with errors less than 10 %”. An important work on the topic has recently been published by the research group of professor Magelli,<sup>41</sup> who discusses the applicability boundaries of the same methods and comes to similar and complementary conclusions as the articles cited above.

For better understanding of the mass transfer in agitated fermenters, we wish to describe the dependencies of transport characteristics on vessel/impeller size, and discuss and experimentally check how to measure the  $k_L a$  in a pilot-plant vessel to obtain the data properly separated from other independent parameters as is, for instance, the gas bubbles mixing time. The  $k_L a$  data measured in the pilot-plant fermenter will be presented, as well as the correlations based on them. Finally, the correlations will be given based on the pilot-plant data together with the laboratory data, which could be suitable for scaling up.

## 2. Theoretical

### 2.1. Process parameters dependence on vessel size

For many years the assumption of the same energy dissipation intensity per liquid volume is considered as the basic requirement for duplicating liquid film controlled mass transfer in scale-up (Miller)<sup>32</sup>. The mass transfer coefficient  $k_L$  combined with the interfacial area  $a$  is experimentally determined in the form of the volumetric mass transfer coefficient  $k_L a$ . Even if the theory of isotropic turbulence is accepted (i.e., the same  $k_L$  under the same dissipation intensity is supposed), the question remains, what is the dependency of  $a$  on the vessel scale when the dissipation intensity is constant.

In our previous work<sup>33</sup> we reported the differences in the behaviour of the relative power down under aeration (the ratio of the impeller power under aeration to the ungassed impeller power) in vessels of different size. The impeller power changes differently with the gas flow rate depending on the vessel scale, which is a result of different amounts of gas passing through the respective impeller region. In connection with the gas amount in the impeller region, the interfacial area  $a$  is also supposed to depend on the vessel scale. Therefore, any parameter proportional to the amount of gas engaged in the impeller region in dependency on the impeller size (vessel scale) should be used.

Gas is drawn into the impeller rotational area by recirculated liquid. The liquid flow rate in the recirculation loop is proportional to the impeller blade circumferential velocity (impeller tip speed)  $\sim fD$ . The differences in the amount of gas engaged in recirculation loops reflect in different values of relative power down under aeration,  $P/P_U$ . The suitable parameters considered in the correlations could be the relative impeller power down under aeration or, directly, the circumferential velocity of impeller blades. To judge the suitability of the parameter  $fD$ , let us analyse its change with the vessel scale. For the same impeller energy dissipa-



tion rate  $P$  ( $P = P_{\text{imp}}/V_L \sim \beta D^5/D^3 = \beta^3 D^2$ ) in the vessels of different scale, we can write:

$$f_{\text{small}}^3 D_{\text{small}}^2 = \left[ \frac{P_{\text{imp}}}{V_L} \right] = f_{\text{large}}^3 D_{\text{large}}^2 \quad (8)$$

The dependencies of the impeller frequency  $f$  and of the circumferential impeller velocity  $fD$  on the vessel scale can be expressed rearranging equation (8):

$$f_{\text{large}} = f_{\text{small}} \left( \frac{D_{\text{small}}}{D_{\text{large}}} \right)^{2/3} \quad (9)$$

$$f_{\text{large}} D_{\text{large}} = f_{\text{small}} D_{\text{small}} \left( \frac{D_{\text{large}}}{D_{\text{small}}} \right)^{1/3} \quad (10)$$

According to equation (9), the impeller frequency is lower under the same impeller power density in the large vessel. On the other hand, according to equation (10), the impeller circumferential velocity (and also the dispersion velocity in the recirculation loop) is higher in the large vessel and, therefore, gas bubbles are engaged in the recirculation loops more intensively. From equation (10), the higher impeller circumferential velocity results for the pilot-plant vessel of inner diameter 0.6 m by 27 % compared to the laboratory vessel of i.d. 0.29 m and by 44 % higher compared to the laboratory vessel of i.d. 0.2 m, when constant  $D/D_T$  ratio is supposed.

## 2.2. The real influence of $k_L a$ value on concentration-time profile in Classical Dynamic Method

The degree of the  $k_L a$  distortion can be illustrated by quantifying how the mass transfer and the gas residence time in the gas hold-up affect the oxygen concentration-time profile, from which the  $k_L a$  is evaluated. To quantify the effect, we will use the simple model of perfectly mixed both liquid and gas phase described by the balances:

$$\frac{dc_L}{dt} = k_L a \cdot (c_L - c_L^*) \quad (11a)$$

and

$$\frac{dc_G}{dt} = \frac{c_{G,\text{in}} - c_G}{\tau_G} \quad (12a)$$

Let us assume oxygen concentration profiles normalized from 1 to 0. If the oxygen concentration changed immediately in the whole gas hold-up volume, the concentration-time profile in liquid saturated by oxygen according to the gas-liquid mass transfer would be described as:

$$c_L = e^{-k_L a t} \quad (11b)$$

and the oxygen concentration profile in perfectly mixed gas after concentration step change at gas inlet is:

$$c_G = e^{-(t/\tau_G)} \quad (12b)$$

These two processes can be combined using the convolution

$$S_{O_2}(t) = \int_0^t c_L(\tau) \cdot \frac{dc_G}{d\tau}(t-\tau) d\tau \quad (13)$$

which gives the shape

$$S_{O_2}(t) = \int_0^t e^{-k_L a \tau} \left( -\frac{1}{\tau_G} e^{-\frac{t-\tau}{\tau_G}} \right) d\tau \quad (14)$$

and after integration per partes

$$S_{O_2}(t) = \left( \frac{1}{1 - k_L a \cdot \tau_G} \right) e^{-k_L a t} + \left( 1 - \frac{1}{1 - k_L a \cdot \tau_G} \right) e^{-t/\tau_G} \quad (15)$$

To simplify the equation formally, we will introduce the “weighting”  $w_{MT}$  for the measure of the effect of the gas-liquid mass transfer coefficient on the liquid concentration profile .

$$S_{O_2}(t) = w_{MT} e^{-k_L a t} + (1 - w_{MT}) e^{-t/\tau_G} \quad (16)$$

Using these equations, we can quantify the degree of the  $k_L a$  effect on the resulting liquid oxygen concentration-time profile,  $S_{O_2}(t)$ . At the medium gas superficial velocity 4.24 mm s<sup>-1</sup> used in this work, for the values of the parameters typical for low mixing intensity (corresponding to the impeller power  $\approx 100 \text{ W m}^{-3}$ )  $k_L a = 0.008 \text{ s}^{-1}$  and  $\varepsilon_G = 0.01$  we obtain the weighting  $w_{MT} = 1.01$  for the mass transfer effect and  $(1 - w_{MT}) = -0.01$  for the gas hold-up washout effect. Meaning that, under low mixing intensity the  $k_L a$  value really determines the  $S_{O_2}(t)$  shape, while the effect of gas hold-up washout is negligible. On the contrary, for the typical values of parameters under high mixing intensity (corresponding to the impeller power  $\approx 6 \text{ kW m}^{-3}$ )  $k_L a = 1 \text{ s}^{-1}$  and  $\varepsilon_G = 0.2$  we obtain  $w_{MT} = -0.03$  for the mass transfer effect and  $(1 - w_{MT}) = 1.03$  for the gas hold-up washout effect. Under these conditions the effect of the exact value of gas-liquid mass transfer coefficient on the shape is negligible, because a slower phenomenon, the gas hold-up washout, controls the liquid concentration-time profile.

## 3. Experimental

### 3.1. Apparatus

Experiments were performed in a cylindrical dished-bottom vessel (internal diameter  $D_T = 0.6 \text{ m}$ ) equipped with four longitudinal baffles  $D_T/10$  thick. Single-, double-, and triple-Rushton Turbine (diameter  $D_T/3$ ) on a common shaft were used. The bottom-impeller clearance was 0.26 m, while inter-impeller clearance in the multiple-impeller configurations was equal to the diameter of the vessel.

Depending on the pressure level required in the vessel, the gas output from the vessel was fed either directly into the atmosphere or through the manostat. To measure the oxygen concentration in each impeller region, oxygen probes were installed slightly above the level of the impellers in each stage. Membrane-covered polarographic oxygen probes with fast response times (with the time constant approximately 1.2 s<sup>-1</sup> for 8  $\mu\text{m}$  thick polypropylene membranes) were used. Experimental details are described in *T. Moucha et al.*<sup>33</sup>

### 3.2. Impeller power and gas hold-up

The impeller power was measured using the strain gauge fixed on the shaft. The net torque, proportional to the impeller power was calculated as the difference between the torque measured under specific operating conditions and the torque measured in the empty vessel (resulting from friction in the bearings). The density power of impellers was calculated both for gassed ( $P$ ) and ungassed ( $P_U$ ) conditions.

The total specific power, dissipated under aeration ( $P_{tot}$ ), is equal to the sum of the impeller power  $P$  and the gas expansion energy

$$P_{tot} = P + \rho_L g v_s \quad (17)$$

Gas hold-up was determined from the difference of the level of the aerated and of the ungassed mechanically agitated liquids.

### 3.3. Mass transfer coefficient

#### 3.3.1. Classical Dynamic Method

The experimental technique comprises step concentration change at the gas inlet. The oxygen concentration in liquid is then recorded as the response to the concentration disturbance in gas. In one experiment, the input gas is exchanged with a new one with a different oxygen concentration after the oxygen concentration in liquid reached the steady-state value, equilibrium to the gas. The liquid oxygen concentration-time profile is then recorded until the new steady state is reached.

The experiments were performed in single-impeller vessel with Rushton Turbine, using the non-coalescent batch (0.5 M  $\text{Na}_2\text{SO}_4$  aqueous solution) and air with nitrogen as gas phases to be interchanged. The superficial gas velocities used were 2.12 and 4.24  $\text{mm s}^{-1}$ . Impeller frequencies ranged from 2.5 to 10  $\text{s}^{-1}$ . The batch temperature was maintained at  $20 \pm 0.2$  °C.

Using the least squares fitting technique with  $k_L a$  as a parameter, the model responses of oxygen absorption were fitted onto the experimental probe responses. In this evaluation model, we assumed the gas and liquid phases perfectly mixed, so equation 16 was used with the  $k_L a$  value as the optimization parameter. The oxygen probe dynamics has been supposed sufficiently fast to be neglected in the Classical Dynamic Method experiments. The oxygen concentration change in liquid is slow in this experimental technique due to the slow gas concentration change when the gas hold-up is washed out.

#### 3.3.2. Dynamic Pressure Method

The principle of the Dynamic Pressure Method, DPM, lies in recording of the responses of oxygen probes in each stage (impeller region) of the vessel after a pressure increase (15 kPa) inside the vessel. The rapid pressure change was realized by injecting extra gas above the liquid level. Experiments were performed in a 0.5 M sodium sulphate solution representing a non-coalescent batch. The superficial gas velocities used were 2.12, 4.24 and 8.48

$\text{mm s}^{-1}$ . Impeller frequencies ranged from 2.5 to 10  $\text{s}^{-1}$ . The batch temperature was maintained at  $20 \pm 0.2$  °C.

Using the least squares fitting technique with  $k_L a$  as a parameter, the model responses of the simultaneous absorption of oxygen and nitrogen were fitted onto the experimental probe responses. The details on the experimental technique and the evaluation procedure in the DPM were described earlier.<sup>29,34</sup>

## 4. Results

### 4.1. Pilot plant data

#### 4.1.1. Impeller power

The power of impellers has been described in the dependency on the impeller frequency and gas superficial velocity by the equation:

$$P = K_1 f^{K_2} v_s^{K_3} \quad (18)$$

The empirical parameters  $K_1$ ,  $K_2$  and  $K_3$  and standard deviations of equation (18) are given in Table 2.

Table 2 – Constants of the equation  $P = K_1 f^{K_2} v_s^{K_3}$  describing the impeller power dependency on process parameters in the pilot-plant vessel in single-, double-, and triple-impeller configuration (1RT, 2RT and 3RT)

Tablica 2 – Konstante jednačbe  $P = K_1 f^{K_2} v_s^{K_3}$  opisuju ovisnost snage miješala u reaktorskim posudama o procesnim parametrima u poluindustrijskom postrojenju u jedno-, dvo- i tro-miješalnoj konfiguraciji (1RT, 2RT i 3RT)

| Number of impellers<br>Broj miješala | $K_1$ | $K_2$ | $K_3$ | $\sigma / \%$ |
|--------------------------------------|-------|-------|-------|---------------|
| 1RT                                  | 0.84  | 2.91  | -0.38 | 11            |
| 2RT                                  | 1.94  | 2.92  | -0.27 | 10            |
| 3RT                                  | 1.63  | 2.84  | -0.33 | 5             |

#### 4.1.2. Gas hold-up

The gas hold-up dependency on the impeller power input and gas superficial velocity has been described by the equation

$$\varepsilon_G = K_1 P^{K_2} v_s^{K_3} \quad (19)$$

for which the  $K_1$ ,  $K_2$ ,  $K_3$ , and standard deviations given in Table 3 were found.

#### 4.1.3. Volumetric mass transfer coefficient

##### 4.1.3.1. Results of the Classical Dynamic Method

Fitting the experimental profile to the model of perfectly mixed gas and liquid (equation (16)) gave the  $k_L a$  values rising to unrealistically high values (in the order of tens and hundreds of  $\text{s}^{-1}$ ) at higher mixing intensities. Instead of such  $k_L a$  values, we rather show the sensitivity analysis.

Table 3 – Constants of the equation  $\varepsilon_G = K_1 P^{K_2} v_s^{K_3}$  describing the gas hold-up dependency on process parameters in the pilot-plant vessel in single-, double-, and triple-impeller configuration (1RT, 2RT and 3RT)

Tablica 3 – Konstante jednadžbe  $\varepsilon_G = K_1 P^{K_2} v_s^{K_3}$  opisuju ovisnost zadržavanja plina u reaktorskim posudama o procesnim parametrima u poluindustrijskom postrojenju u jedno-, dvo- i tro-miješalnoj konfiguraciji (1RT, 2RT i 3RT)

| Number of impellers<br>Broj miješala | $K_1$ | $K_2$ | $K_3$ | $\sigma / \%$ |
|--------------------------------------|-------|-------|-------|---------------|
| 1RT                                  | 0.061 | 0.47  | 0.58  | 11            |
| 2RT                                  | 0.080 | 0.50  | 0.59  | 23            |
| 3RT                                  | 0.65  | 0.25  | 0.72  | 18            |

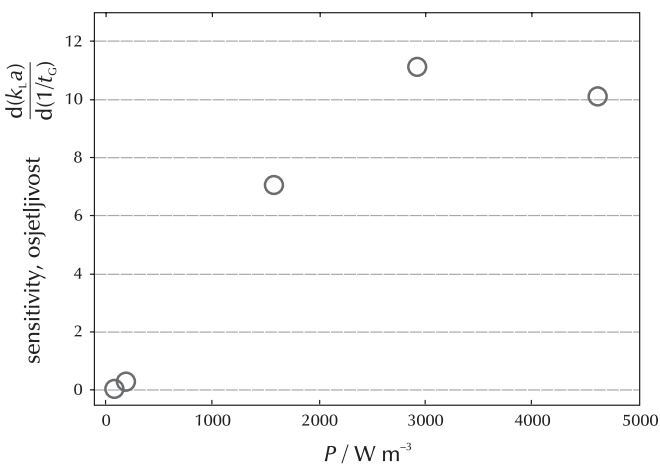


Fig. 1 – Sensitivity of  $k_La$  evaluated by the Classical Dynamic Method to the inaccuracies in the gas residence time

Slika 1 – Osjetljivost  $k_La$  procijenjena klasičnom dinamičkom metodom netočnosti u vremenu zadržavanja plinovite faze

The sensitivity in Fig. 1 was obtained by the evaluation of the change in  $k_La$  (by fitting the equation 16 to the experimental liquid oxygen concentration-time profile) after a small change (5 % of its value) in the gas hold-up. The sensitivity value was obtained as the ratio of the difference in  $k_La$  to the difference in the gas residence time during the small change in gas hold-up values (numerical derivative). In the region of high gas-liquid mass transfer intensities, the model response is much more sensitive to inaccuracies in gas-hold-up values or gas flowrates (in Fig. 1 in terms of the gas residence time  $\tau_c$ ) than to the  $k_La$  value. Therefore, the change in process parameters within the range of experimental uncertainty can change the resulting  $k_La$  values by multiples.

For the reason mentioned above, we evaluated the  $k_La$  data using the model of oxygen concentration response in perfectly mixed liquid to the step concentration change in gas neglecting the gas hold-up washout. We fitted the experimental liquid oxygen concentration-time profiles to the equation (11) with the  $k_La$  as the optimization parameter. Such evaluation of  $k_La$  in the Classical Dynamic Method is commonly used in literature.<sup>35,36</sup> The results are shown in Fig. 2.

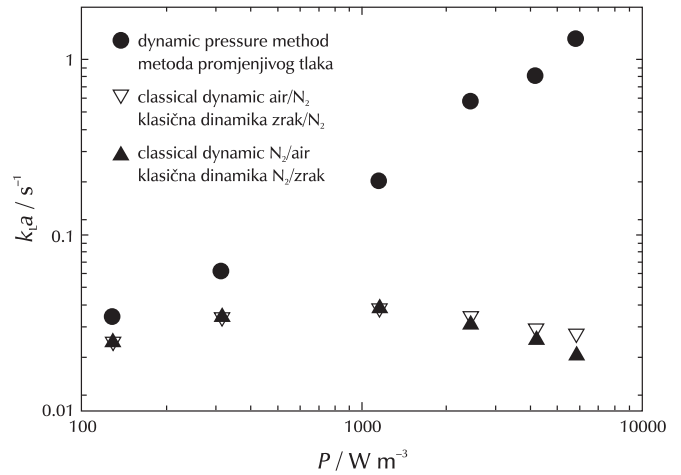


Fig. 2 – Comparison of  $k_La$  data measured by the classical dynamic method with those measured by the dynamic pressure method (DPM)

Slika 2 – Usporedba podataka  $k_La$  izmjerenih klasičnom dinamičkom metodom s podacima određenim metodom dinamičkog tlaka (DPM)

There is a principled distinction between the  $k_La$  data obtained using both methods. Fig. 2 shows the principle change in the dependency of  $k_La$  measured by classical dynamic method: from the rising trend at low impeller power to the decreasing trend at high impeller power, where the  $k_La$  are distorted by the effect of the gas hold-up flushing out, the reason for which has been discussed in section 2.2. Thus, the results obtained using the data from the pilot-plant vessel confirm the conclusions of other papers (obtained for laboratory vessels) that this simply realizable method cannot be used in further study.

#### 4.1.3.2. Results of the Dynamic Pressure Method

The volumetric mass transfer coefficients for pilot-plant vessel are presented in the form of the average values for the whole vessel with  $N$  impellers:

$$k_La = \frac{1}{N} \sum_{i=1}^N k_{L,i}a_i \quad (20)$$

where  $k_{L,i}a_i$  are the values measured in individual stages (individual impeller regions) of multiple-impeller vessel. The  $k_{L,i}a_i$  values have been evaluated by the procedure mentioned in the section 3.3.2.

First, we verified if the DPM provides the physically correct  $k_La$  data also in the pilot-plant scale and under high  $k_La$  values corresponding with non-coalescent batch. As proof of physical accuracy, which means the proper  $k_La$  separation from the driving force of the absorption, we considered the agreement of the data obtained by the absorption of air with those obtained by pure oxygen absorption (see Fig. 3).

Further, we present the  $k_La$  values for the pilot-plant vessel in the dependency on the total power input  $P_{tot}$  and the superficial gas velocity  $v_s$ :

$$k_La = 2.27 \cdot 10^{-3} P_{tot}^{0.96} v_s^{0.33} \quad (\sigma = 27) \quad (21)$$

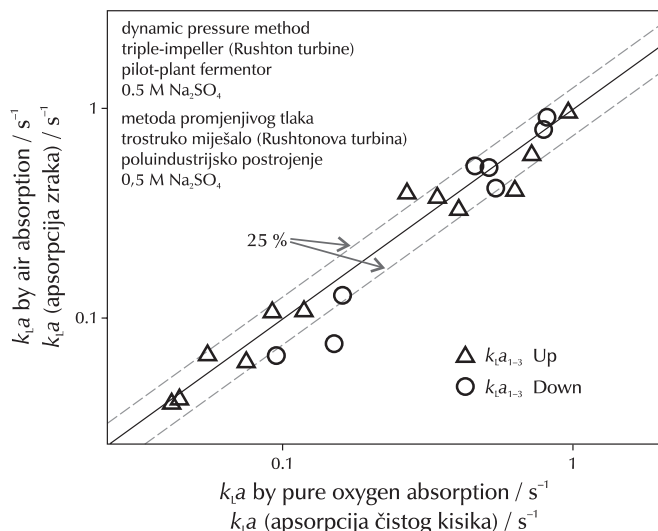


Fig. 3 – DPM results: Comparison of  $k_La$  data measured by air absorption with those measured by pure oxygen absorption. “ $k_{L,a1-3}$  Up” and “ $k_{L,a1-3}$  Down” are the average values for the whole triple-impeller vessel measured by the total pressure increase and the total pressure decrease, respectively

Slika 3 – Rezultati DPM-a: usporedba podataka  $k_La$  mjerenih apsorpcijom zraka s podatcima mjerenim apsorpcijom čistog kisika. “ $k_{L,a1-3}$  Up” i “ $k_{L,a1-3}$  Down” su prosječne vrijednosti za cijeli reaktor s trostrukim miješalom mjerene ukupnim porastom tlaka odnosno ukupnim smanjenjem tlaka

The power factor of  $P_{tot}$  found for the pilot-plant fermenter is consistent with the literature data presented in the Introduction.

The data are shown in Fig. 4 and the correlation closeness for non-coalescent batch (being of a higher standard deviation compared with the coalescent batch data) is illustrated in Fig. 5.

**4.2. Various scale data – vessel scale effect**

To study the dependency of the  $k_La$  values on vessel size, we included our earlier data for two laboratory scale vessels (of standard geometry with each impeller region height equal to vessel diameter). The data from the laboratory vessels of inner diameters 0.19 m and 0.29 m were originally presented in<sup>27</sup> and,<sup>37,38</sup> respectively. All the  $k_La$  data used hereinafter were obtained by the dynamic pressure method.

To study how to reach the best fit of  $k_La$  data using a scalable correlation, we used three correlation shapes. Together with the classic correlation based on the theory of isotropic turbulence in the shape

$$k_La = K_1 P_V^{K_2} v_s^{K_3} \tag{2}$$

the correlations with the additional terms

- i) of the relative power down under aeration  $P/P_U$  and
- ii) of the circumferential velocity of impeller blades  $fD$

have also been used. The additional terms have been introduced to involve the differences in the behaviour of impellers in vessels of different size. Further, we tried both to

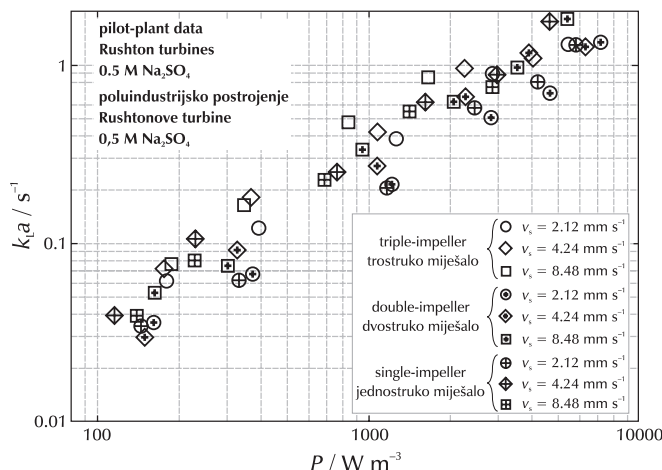


Fig. 4 – Values of  $k_La$  measured by the DPM in the pilot-plant fermenter

Slika 4 – Vrijednosti  $k_La$  mjerene metodom DPM u fermentoru poluindustrijskog postrojenja

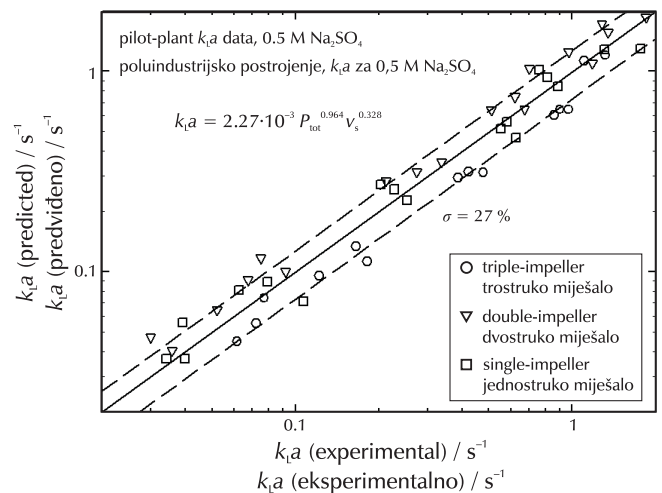


Fig. 5 – Correlation of mass transfer coefficients measured in the pilot-plant vessel

Slika 5 – Korelacija koeficijena prijenosa tvari mjerenih u reaktorskim posudama poluindustrijskog postrojenja

treat the average  $k_La$  data for whole multiple-impeller vessels and separate the data for individual impeller regions of the vessel.

As the criterion to assess the correlation closeness we used the standard deviation of the differences between experimental and predicted  $k_La$ .

**4.2.1. Average  $k_La$  for whole vessels**

The  $k_La$  data gathered from the experiments performed in vessels of 3 different scales using single-, double-, and triple-impeller configurations lead to the following correlation shapes:

$$k_La = 4.17 \cdot 10^{-4} P_{tot}^{1.17} v_s^{0.34} \quad (\sigma = 47) \tag{22}$$

$$k_La = 2.88 \cdot 10^{-3} P_{tot}^{1.18} v_s^{0.64} (P/P_U)^{0.85} \quad (\sigma = 41) \tag{23}$$

$$k_La = 3.12 \cdot 10^{-2} P_{tot}^{0.47} v_s^{0.19} (fD)^{1.85} \quad (\sigma = 29) \tag{24}$$



By the involvement of the additional terms, the standard deviation decreased significantly, especially in the case of the impeller circumferential velocity. The correlations of experimental  $k_L a$  data by the equations (22), (23), and (24) are illustrated in Figs. 6, 7, and 8, respectively.

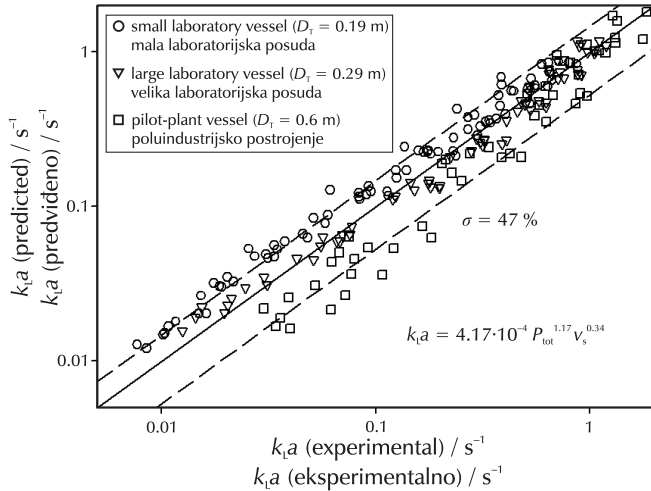


Fig. 6 – Average  $k_L a$  data correlated by eq. (22)  
Slika 6 – Prosječni podatci  $k_L a$  u korelaciji s jednadžbom (22)

The power input per unit liquid volume is often considered as the variable, which should be maintained constant in the agitated vessel design to keep the desired value of  $k_L a$ . In Fig. 6 we can see, however, the differences up to 100 % between the experimental  $k_L a$  for different vessel scales under the same  $P_{tot}$  and  $v_s$ , i.e., at single value of  $k_{L a, predicted}$ . This finding emphasizes the need of seeking an additional parameter, which would improve the accuracy in the maintenance of the desired  $k_L a$  values in scale-up.

The term of relative impeller power down under aeration brought a slight decrease in the standard deviation from 47 to 41 %.

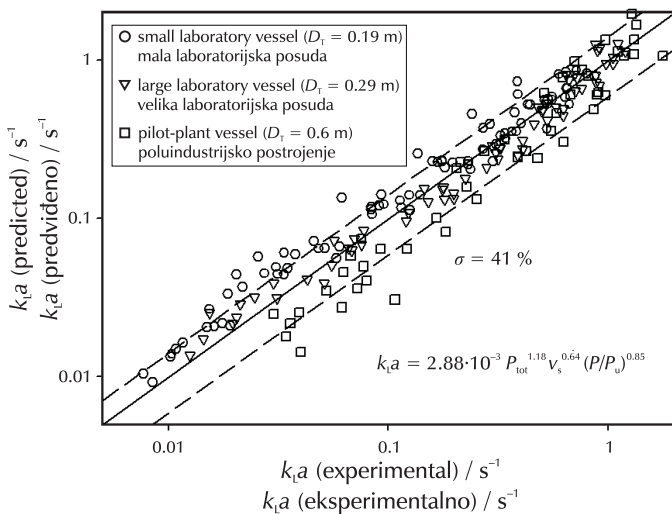


Fig. 7 – Average  $k_L a$  data correlated by eq. (23)  
Slika 7 – Prosječni podatci  $k_L a$  u korelaciji s jednadžbom (23)

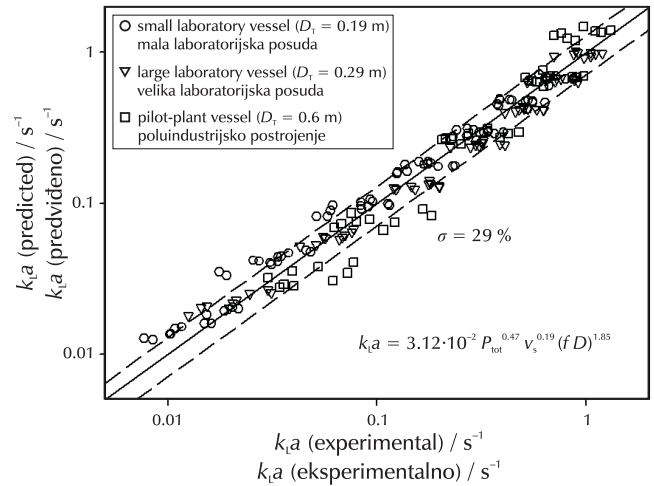


Fig. 8 – Average  $k_L a$  data correlated by eq. (24)  
Slika 8 – Prosječni podatci  $k_L a$  u korelaciji s jednadžbom (24)

The lowest standard deviation gave the correlation (24) involving the circumferential impeller velocity term.

#### 4.2.2. Local $k_L a$ data extraction

##### 4.2.2.1. Data treatment

With respect to the different behaviour of the bottom and upper impellers, the values of  $k_{L a, i}$ , which are characteristic for individual stages (impeller regions) of multiple-impeller vessel, have been extracted. The method for extracting the data characteristic for upper stages  $k_{L a_{2-N}}$  is based on our previous finding:<sup>39</sup> we showed that the  $k_L a$  values measured in individual stages are not exactly characteristic ones,  $k_{L a, i}$ , because they are distorted by exchange flows between adjacent impellers. The average values for the whole vessel (calculated according to equation 20) are, however, the same regardless of whether they were calculated from the distorted experimental values or from the characteristic  $k_{L a, i}$ . Exploiting this finding, the characteristic  $k_{L a_{2-N}}$  values for upper stages can be separated as follows:

$$k_{L a_{2-N}} = \frac{N \cdot k_{L a_{1-N}}(\text{multiple impeller}) - k_{L a}(\text{single impeller})}{N - 1} \quad (25)$$

where it is assumed that the bottom stage in a multiple-impeller configuration is characterized by the same local  $k_{L a, i}$  value as the  $k_{L a}(\text{single impeller})$  measured in a single-impeller vessel is.

The values of  $P_{2-N}$  (as well as  $P_{tot(2-N)}$ ) necessary for  $k_{L a_{2-N}}$  correlation were calculated similarly:

$$P_{2-N} = \frac{N \cdot P(\text{multiple impeller}) - P(\text{single impeller})}{N - 1} \quad (26)$$

##### 4.2.2.2. Results of local data

The  $k_{L a_{2-N}}$  data were calculated for all the vessel scales and correlated together, which resulted in the following relations:

$$k_{L a_{2-N}} = 6.01 \cdot 10^{-4} P_{tot(2-N)}^{1.14} v_s^{0.39} \quad (\sigma = 38) \quad (27)$$



$$k_L a_{2-N} = 1.2 \cdot 10^{-3} P_{\text{tot}2-N}^{1.15} v_s^{0.50} \left( \frac{P}{P_U} \right)^{0.35} \quad (\sigma = 37) \quad (28)$$

$$k_L a_{2-N} = 2.38 \cdot 10^{-2} P_{\text{tot}2-N}^{0.57} v_s^{0.27} (fD)^{1.50} \quad (\sigma = 31) \quad (29)$$

The standard deviations are of a similar trend as in the case of the treatment of the average  $k_L a$  data for whole vessels, i.e., the term of the impeller circumferential velocity  $fD$  improved the  $k_L a$  data correlation closeness more significantly than the term of the relative power down under aeration  $P/P_U$ .

The correlations for only single-impeller configurations, which are supposed to be identical to the  $k_L a$  data characteristic for bottom stages of multiple-impeller vessels, resulted in:

$$k_L a_1 = 3.12 \cdot 10^{-4} P_{\text{tot}1}^{1.18} v_s^{0.31} \quad (\sigma = 45) \quad (30)$$

$$k_L a_1 = 4.37 \cdot 10^{-3} P_{\text{tot}1}^{1.19} v_s^{0.68} \left( \frac{P}{P_U} \right)^{1.02} \quad (\sigma = 43) \quad (31)$$

$$k_L a_1 = 1.93 \cdot 10^{-2} P_{\text{tot}1}^{0.49} v_s^{0.15} (fD)^{1.86} \quad (\sigma = 26) \quad (32)$$

We again see the convenience to include the impeller circumferential velocity  $fD$  also for single-impeller data – compare the standard deviation 26 % in eq. (32) with 45 % in eq. (30) and 43 % in eq. (31).

#### 4.2.3. Dimensionless $k_L a$ correlations

The analysis in the previous paragraphs has shown, that it is sufficient to correlate the average  $k_L a$  data for whole vessels (i.e., the correlation closeness is not improved by the separation of  $k_L a$  values for upper and bottom stages) as well as to correlate the data for single, double and triple-impeller together. The suggested dimensionless correlations for average  $k_L a$  for the whole vessel incorporate  $k_L a$  coefficient in the form of the Sherwood number

$$Sh \cdot a \cdot \ell = \frac{k_L a \cdot \ell^2}{D_{O_2}} \quad (33)$$

in dependency on Reynolds number

$$Re = \frac{fD\ell}{\nu_L} \quad (34)$$

where the characteristic velocity is given by the impeller blade circumferential velocity  $fD$ . Through the dimensionless correlations, we tried to improve the closeness of the  $k_L a$  description using the characteristic dimension  $\ell$  both in  $Sh$  and in  $Re$  expressed as the microscale of turbulence defined by Batchelor<sup>40</sup> in terms of liquid viscosity  $\nu_L$  and energy dissipation intensity  $\varepsilon$ :

$$\ell \sim \frac{\nu_L^{3/4}}{\varepsilon^{1/4}} \quad (35)$$

By including the gas superficial velocity normalized by bubble terminal velocity  $v_s/v_t$ , the final shape of the 3-parameter correlation was obtained:

$$\frac{k_L a \cdot \ell^2}{D_{O_2}} = K_1 \left( \frac{fD}{(\varepsilon \nu_L)^{1/4}} \right)^{K_2} \left( \frac{v_s}{v_t} \right)^{K_3} \quad (36)$$

or rewritten using the definitions of dimensionless criteria

$$Sh \cdot a \cdot \ell = K_1 \cdot Re^{K_2} \left( \frac{v_s}{v_t} \right)^{K_3} \quad (37)$$

The bubble terminal velocity was supposed to be constant with the value  $0.27 \text{ m s}^{-1}$  (Kawase and Moo-Young).<sup>9</sup> When the average  $k_L a$  data fitted together for the vessels of all three scales, the correlation with the parameters

$$Sh \cdot a \cdot \ell = 5.35 \cdot 10^{-8} Re^{3.71} \left( \frac{v_s}{v_t} \right)^{-0.019} \quad (\sigma = 43) \quad (38)$$

has been obtained.

To involve the effect of the fermenter scale, the 4-parameter correlation has been used, into which the impeller circumferential velocity normalized by the bubble terminal velocity  $fD/v_t$  has been added. The following parameters and standard deviations have been obtained

$$Sh \cdot a \cdot \ell = 0.016 \cdot Re^{0.30} \left( \frac{v_s}{v_t} \right)^{0.177} \left( \frac{fD}{v_t} \right)^{1.65} \quad (\sigma = 29) \quad (39)$$

Apparently, the addition of the fourth parameter, impeller blade circumferential velocity, improves the correlation closeness significantly regardless of whether the dimensionless form is used or not.

## 5. Conclusions

After we had selected the proper experimental technique for  $k_L a$  measurement in a pilot-plant fermenter, and verified the physical accuracy of its results, we developed the  $k_L a$  correlations in dependency on process parameters. The correlations describe the data obtained from the fermenters of various scales, therefore they are scalable.

The circumferential velocity of impeller blades (tip speed) in terms of  $fD$  revealed itself to be a useful parameter, which significantly improves the closeness of  $k_L a$  correlations. This finding, obtained using a non-coalescent batch, is significant because practically all industrial batches are non-coalescent and, using the extended 4-parameter correlation, the uncertainty in the design of large scale fermenters can be reduced almost from  $1/2$  to  $1/4$  of their total volume. This conclusion holds for average  $k_L a$  data for whole multiple-impeller vessels, as well as for  $k_L a$  data for upper and bottom impellers.

#### ACKNOWLEDGEMENT

Support from the Ministry of Education (MSM 6046137306) is gratefully acknowledged.

**List of abbreviations and symbols****Popis kratica i simbola**

|               |  |                 |   |
|---------------|--|-----------------|---|
| 1             | – value for single-impeller vessel<br>– vrijednost za reakcijsku posudu s jednim miješalom   | $P_{2-N}$       | – impeller power density in upper stages of the vessel, $W m^{-3}$<br>– gustoća snage miješala u gornjim odjeljcima posude, $W m^{-3}$                            |
| 1–N           | – average value for the whole vessel<br>– prosječna vrijednost za cijelu posudu  | $P_{imp}$       | – impeller power, W<br>– snaga miješala, W  |
| 2–N           | – value for upper stages of multiple-impeller vessel<br>– vrijednost za gornje odjeljke posude s više miješala   | $P_{tot}$       | – total power density input, $W m^{-3}$<br>– ukupna gustoća ulazne snaga, $W m^{-3}$  |
| a             | – gas-liquid interfacial area per liquid volume, $m^2 m^{-3}$<br>– omjer ploštine međupovršine plin/kapljevina i obujma kapljevine, $m^2 m^{-3}$                                     | $P_U$           | – ungassed impeller power density, $W m^{-3}$<br>– gustoća snage neareriranog miješala, $W m^{-3}$  |
| $c_G$         | – oxygen concentration in gas, $mol m^{-3}$<br>– koncentracija kisika u plinu, $mol m^{-3}$  | Re              | – Reynolds number<br>– Reynoldsov broj  |
| $c_L$         | – oxygen concentration in liquid, $mol m^{-3}$<br>– koncentracija kisika u kapljevine, $mol m^{-3}$  | $S_{O_2}(t)$    | – liquid oxygen concentration-time profile normalized from 1 to 0<br>– normalizirani (od 1 do 0) vremenski profil koncentracije kisika u kapljevine               |
| $c_L^*$       | – oxygen concentration in liquid equilibrium to gas, $mol m^{-3}$<br>– koncentracija kisika u kapljevine u ravnoteži s plinom, $mol m^{-3}$  | Sh              | – Sherwood number<br>– Sherwoodov broj  |
| D             | – impeller diameter, m<br>– promjer miješala, m  | t               | – time, s<br>– vrijeme, s   |
| $D_{O_2}$     | – oxygen diffusion coefficient in liquid, $m^2 s^{-1}$<br>– difuzijski koeficijent kisika u kapljevine, $m^2 s^{-1}$   | $t_G$           | – gas residence time in the gas hold-up, s<br>– vrijeme zadržavanja plina u reaktoru, s   |
| $D_T$         | – vessel diameter, m<br>– promjer posude, m  | $V_L$           | – liquid volume, $m^3$<br>– volumen kapljevine, $m^3$   |
| f             | – impeller frequency, $s^{-1}$<br>– frekvencija miješala, $s^{-1}$   | $v_s$           | – gas superficial velocity, $m s^{-1}$<br>– površinska brzina plina, $m s^{-1}$   |
| g             | – gravitational constant, $m s^{-2}$<br>– gravitacijska konstanta, $m s^{-2}$  | $v_t$           | – bubble terminal velocity, $m s^{-1}$<br>– konačna brzina mjehurića, $m s^{-1}$  |
| $k_L$         | – mass transfer coefficient, $m s^{-1}$<br>– koeficijent prijenosa tvari, $m s^{-1}$   | $w_{MT}$        | – weighting coefficient for $k_L a$ effect on $S_{O_2}(t)$<br>– težinski faktor učinka $k_L a$ na $S_{O_2}(t)$  |
| $k_L a$       | – volumetric mass transfer coefficient, $s^{-1}$<br>– obujamski koeficijent prijenosa tvari, $s^{-1}$  | $\varepsilon$   | – energy dissipation intensity, $W kg^{-1}$ ; $\varepsilon = P_{tot} / \rho_L$<br>– intenzitet rasipanja energije, $W kg^{-1}$ ; $\varepsilon = P_{tot} / \rho_L$ |
| $k_L a_i$     | – volumetric mass transfer coefficient characteristic for $i^{th}$ stage/impeller region, $s^{-1}$<br>– obujamski koeficijent prijenosa tvari $i$ -tog odjeljka, $s^{-1}$            | $\varepsilon_G$ | – gas hold-up in the dispersion volume fraction<br>– obujamski udjel plina zadržanog u disperziji   |
| $k_L a_{k-N}$ | – average volume mass transfer coefficient from $k^{th}$ to $N^{th}$ stage, $s^{-1}$<br>– prosječni obujamski koeficijent prijenosa tvari od $k$ -tog do $N$ -tog odjeljka, $s^{-1}$ | $\nu_L$         | – liquid phase kinematic viscosity, $m^2 s^{-1}$<br>– kinematička viskoznost kapljevite faze, $m^2 s^{-1}$  |
| $K_i$         | – empirical constants in the correlations of transport characteristics<br>– empirijska konstanta korelacije transportnih svojstava   | $\rho_L$        | – liquid phase density, $kg m^{-3}$<br>– gustoća kapljevite faze, $kg m^{-3}$   |
| $\ell$        | – Batchelor length scale, m<br>– Batchelorovo mjerilo duljine, m   | $\sigma$        | – standard deviation<br>– standardna devijacija   |
| N             | – number of impellers in the vessel<br>– broj miješala u posudi  | $\tau_G$        | – gas residence time in the gas hold-up, s<br>– vrijeme zadržavanja plina u reaktoru, s   |
| P             | – impeller power density (power per liquid volume), $W m^{-3}$<br>– gustoća snage miješala (omjer snage i obujma kapljevine), $W m^{-3}$   | CDM             | – classical dynamic method<br>– klasična dinamička metoda   |
|               |  | CFD             | – computational fluid dynamics<br>– računalna dinamika fluida   |
|               |  | DPM             | – dynamic pressure method<br>– metoda promjenjivog tlaka  |
|               |  | i.d.            | – inner diameter, m<br>– unutarnji promjer, m   |
|               |  | OTR             | – oxygen transfer rate<br>– brzina prijenosa kisika   |

## References

## Literatura

1. P. R. Gogate, A. B. Pandit, Survey of measurement techniques for gas-liquid mass transfer coefficient in bioreactors, *Biochem. Eng. J.* **4** (1999) 7–15.
2. N. J. Kraakman, J. Rocha-Rios, M. C. M. van Loosdrecht, Review of mass transfer aspects for biological gas treatment, *Appl. Microbiol. Biotechnol.* **91** (2011) 873–886.
3. K. Takahashi, A. W. Nienow, Bubble Sizes and Coalescence Rates in an Aerated Vessel Agitated by a Rushton Turbine, *J. Chem. Eng. Japan* **25** (1993) 536–542.
4. W. J. Timson, C. G. Dunn, Mechanism of Gas Absorption from Bubbles Under Shear, *Ind. Eng. Chem.* **52** (1960) 799–802.
5. T. Okawa, K. Yoneda, S. Zhou, New Interfacial Drag Force Model Including Effect of Bubble Wake, *J. Nuclear Sci. Technol.* **36** (1999) 1030–1040.
6. L. A. Del Castillo, S. Ohnishi, R. G. Horn, Inhibition of bubble coalescence: Effects of salt concentration and speed of approach, *J. Colloid Interface Sci.* **356** (2011) 316–324.
7. M. A. R. Talaia, Terminal Velocity of a Bubble Rise in a Liquid Column, *World Acad. Sci., Eng. Technol.* **28** (2007) 264–268.
8. M. J. Prince, H. W. Blanch, Bubble Coalescence and Break-Up in Air-Sparged Bubble Columns, *AIChE J.* **36** (1990) 1485–1499.
9. Y. Kawase, M. Moo-Young, Volumetric mass transfer coefficient in aerated stirred tank reactors with Newtonian and non-Newtonian media, *Chem. Eng. Res. Des.* **66** (1988) 284–288.
10. P. Ranganathan, S. Sivaraman, Investigations on hydrodynamics and mass transfer in gas-liquid stirred reactor using computational fluid dynamics, *Chem. Eng. Sci.* **66** (2011) 3108–3124.
11. S. S. Alves, C. I. Maia, J. M. T. Vasconcelos, Gas-liquid mass transfer coefficient in stirred tanks interpreted through bubble contamination kinetics, *Chem. Eng. Proc.* **43** (2004) 823–830.
12. M. Martin, F. J. Montes, M. A. Galan, Physical explanation of the empirical coefficients of gas-liquid mass transfer equations, *Chem. Eng. Sci.* **64** (2009) 410–425.
13. K. van't Riet, Review of measuring methods and results in non-viscous gas-liquid mass transfer in stirred vessels, *Ind. Eng. Chem., Proc. Des. Dev.* **18** (1979) 357–364.
14. H. Herbst, A. Schumpe, W. D. Deckwer, Xanthan Production in Stirred Tank Fermenters: Oxygen Transfer and Scale-up, *Chem. Eng. Technol.* **15** (1992) 425–434.
15. M. Nocentini, D. Fajner, G. Pasquali, F. Magelli, Gas-liquid mass transfer and hold-up in vessels stirred with multiple Rushton turbines: Water and Water-glycerol solutions, *Ind. Eng. Chem. Res.* **32** (1993) 19–26.
16. C. W. Robinson, C. R. Wilke, Oxygen Absorption in Stirred Tanks: A Correlation for Ionic Strength Effects, *Biotechnol. Bioeng.* **15** (1973) 755–782.
17. V. Linek, V. Vacek, P. Beneš, A critical review and experimental verification of the correct use of the Dynamic Method for the determination of Oxygen Transfer in aerated agitated vessels to water, electrolyte solutions and viscous liquids, *Chem. Eng. J.* **34** (1987) 11–34.
18. M. S. Puthli, V. K. Rathod, A. B. Pandit, Gas-liquid mass transfer studies with triple impeller system on a laboratory scale bioreactor, *Biochem. Eng. J.* **23** (2005) 25–30.
19. A. G. Pedersen, H. Andersen, J. Nielsen, J. Villadsen, A Novel Experimental Technique Based on  $^{85}\text{Kr}$  for Quantification of Gas-Liquid Mass Transfer in Bioreactors, *Chem. Eng. Sci.* **49** (1994) 803–810.
20. Y. Imai, H. Takeji, M. Matsumura, A simple  $\text{Na}_2\text{SO}_3$  feeding method for  $k_La$  measurement in large-scale fermenters, *Biotechnol. Bioeng.* **29** (1987) 982–993.
21. V. Linek, P. Beneš, O. Holeček, Correlation for Volumetric Mass Transfer Coefficient in Mechanically Agitated Aerated Vessel for Oxygen Absorption in Aqueous Electrolyte Solutions, *Biotechnol. Bioeng.* **32** (1988) 482–490.
22. T. Poizat, C. Jallut, A. Accary, J. Lieto, A novel experimental technique for measurement of mass transfer between liquids and gas bubbles in agitated vessels: application to highly viscous liquids, *Chem. Eng. J.* **48** (1992) 41–48.
23. R. Puskeiler, D. Weuster-Botz, Combined sulphite method for the measurement of the oxygen transfer coefficient  $k_La$  in bioreactors, *J. Biotechnol.* **120** (2005) 430–438.
24. D. Pinelli, A phenomenological model for the gas phase flowing high-aspect-ratio stirred vessels: the role of small bubbles in non-coalescent and moderately viscous liquids, *Chem. Eng. Sci.* **60** (2005) 2239–2252.
25. P. Havelka, V. Linek, J. Sinkule, J. Zahradník, M. Fialová, Hydrodynamic and mass transfer characteristics of ejector loop reactors, *Chem. Eng. Sci.* **55** (2000) 535–549.
26. N. Midoux, A. Laurent, J. C. Charpentier, Limits of the chemical method for the determination of physical mass transfer parameters in mechanically agitated gas-liquid reactors, *AIChE J.* **26** (1980) 157–161.
27. V. Linek, T. Moucha, J. Sinkule, Gas-liquid mass transfer in vessels stirred with multiple impellers-Part I: Gas-liquid mass transfer characteristics in individual stages, *Chem. Eng. Sci.* **51** (1996) 3203–3212.
28. P. Havelka, T. Moucha, J. Sinkule, V. Linek, Chemical dynamic method for measuring  $k_La$  in gas-liquid dispersions, *Chem. Eng. Commun.* **168** (1998) 97–110.
29. V. Linek, P. Beneš, J. Sinkule, T. Moucha, Non-ideal pressure step method for  $k_La$  measurement, *Chem. Eng. Sci.* **48** (1993) 1593–1599.
30. R. I. Carbajal, A. Tecante, On the applicability of the dynamic pressure step method for  $k_La$  determination in stirred Newtonian and non-Newtonian fluids, culture media and fermentation broths, *Biochem. Eng. J.* **18** (2004) 185–192.
31. F. Scargiali, A. Busciglio, F. Grisafi, A. Brucato, Simplified dynamic pressure method for  $k_La$  measurement in aerated bioreactors, *Biochem. Eng. J.* **49** (2010) 165–172.
32. D. N. Miller, Scale-up of Agitated Vessels Gas-Liquid Mass Transfer, *AIChE J.* **20** (1974) 445–453.
33. T. Moucha, V. Linek, K. Erokhin, F. J. Rejl, M. Fijasová, Improved power and mass transfer correlations for design and scale-up of multiple-impeller gas-liquid contactors, *Chem. Eng. Sci.* **64** (2009) 598–604.
34. V. Linek, J. Sinkule, The influence of gas and liquid axial dispersion on determination of  $k_La$  by dynamic method, *Trans. Inst. Chem. Eng.* **69A** (1991) 308–312.
35. F. Garcia-Ochoa, E. Gomez, Mass transfer coefficient in stirred tank reactors for xanthan gum solutions, *Biochem. Eng. J.* **1** (1998) 1–10.
36. U. Jordan, A. Schumpe, The gas density effect on mass transfer in bubble columns with organic liquids, *Chem. Eng. Sci.* **56** (2001) 6267–6272.
37. T. Moucha, V. Linek, E. Prokopová, Gas hold-up, mixing time and gas-liquid volumetric mass transfer coefficient of various

- multiple-impeller configurations: Rushton turbine, pitched blade and techmix impeller and their combinations, *Chem. Eng. Sci.* **58** (2003) 1839–1846.
38. M. Fugasová, V. Linek, T. Moucha, Mass transfer correlations for multiple-impeller gas-liquid contactors. Analysis of the effect of axial dispersion in gas and liquid phases on “local”  $k_L a$  values measured by the dynamic pressure method in individual stages of the vessel, *Chem. Eng. Sci.* **62** (2007) 1650–1669.
39. T. Moucha, V. Linek, J. Sinkule, Effect of liquid axial mixing on local  $k_L a$  values in individual stages of multiple-impeller vessel, *Collect. Czech. Chem. Commun.* **63** (1998) 2103–2113.
40. G. K. Batchelor, *The theory of homogeneous turbulence*, Cambridge University Press, Cambridge, 1953.
41. D. Pinelli, Z. Liu, F. Magelli, Analysis of  $K_L a$  Measurement Methods in Stirred Vessels: The Role of Experimental Techniques and Fluid Dynamic Models, *Int. J. Chem. React. Eng.* **8** (2010) Article A115.

### SAŽETAK

#### Projektiranje i uvećanje mjerila biokemijskih reaktora s višestrukim miješalima

L. Labík, T. Moucha\* i M. Kordač

Uređaji za mehaničko miješanje sustava kapljevina-plin često se upotrebljavaju u kemijskoj, prehrambenoj i biokemijskoj industriji kao fermentori i kao reaktori za hidrogeniranje i kloriranje. No u širokoj primjeni takvih reaktora njihov se dizajn ne temelji na kemijsko-inženjerskim podacima te je još uvijek prilično empirijski. Dakle, vrlo je poželjno imati alat za racionalno projektiranje/dizajn uređaja za mehaničko miješanje sustava kapljevina-plin koji se temelji na fundamentalnim kemijsko-inženjerskim parametrima koji su prenosivi i na druge sustave i druge radne uvjete. Usredotočivši se na procese kontrolirane tekućim filmom i primjenjujući podatke iz fermentera različitih mjerila, razvijene su korelacije  $k_L a$  koje su pogodne za uvećanje mjerila.

Najprije se govori o načinu kako utvrditi odgovarajuće eksperimentalne vrijednosti  $k_L a$  koje nisu narušene drugim parametrima kao što je to vrijeme zadržavanja plina. Pokazuje se moguća distorzija eksperimentalnih podataka  $k_L a$  poluindustrijskih postrojenja usporedbom rezultata koji su dobiveni dvjema različitim eksperimentalnim tehnikama. Nadalje, prikazuju se fizički ispravni podatci  $k_L a$  za smjesu (otopinu natrijeva sulfata) u potpunosti bez koalescencije (spajanja). Podatci su prikazani i za laboratorij i za fermentore poluindustrijskih postrojenja. Utvrđuju se procesni parametri – vrijednosti koje su ovisne o mjerilu reaktorske posude, kada djeluju pod istom ulaznom snagom po jedinici obujma i primjenom ovih parametara razvijaju se uobičajene korelacije  $k_L a$  prikladne za opisivanje podataka za različita mjerila reaktorske posude.

Razvijene korelacije smanjuju nesigurnost u predviđanju obujma fermentora industrijskih razmjera s gotovo  $1/2$  do  $1/4$  od svog ukupnog obujma i time omogućuju znatno smanjenje početnih operativnih troškova.

*Institute of Chemical Technology Prague,  
Chemical Engineering Dept.,  
Technická 5, 166 28 Prag 6, Republika Češka*

*Prispjelo 11. listopada 2012.  
Prihvaćeno 4. veljače 2013.*